ALEPH 91-3
PHYSIC 91-3
Levinthal
Bird
17.1.1991

Standard Model Fits of 1990 Data with Expostar

In the past few weeks a complete analysis of the 1990 data sample with the EXPOSTAR fitting program has been completed. The data selection and analysis are outlined here. A comparison of EXPOSTAR with the ALIBABA calculation, interesting for Bhabha scattering is included as Appendix A, and a brief introduction to the inner workings of the EXPOSTAR program is included as Appendix B.

Data Selection and Cuts

The data is derived from the good run selection as it stood in September. Since that time, 15 runs have been degraded due to poor muon identification hardware status. As this does not affect the current analysis we have not rerun the data selection. The hadron data sample is the standard TPC-based selection, and the luminosity selection is the standard method 5 analysis. The numbers of events were provided by J. Wear and J. Harton. The lepton selection can be described as the original common lepton selection (i.e., not based on class 15) with the electron pairs isolated by the Locci/Clifft algorithm. There are a few differences. The two important ones allow this analysis to have a more precisely defined phase space in which the events are distributed: the events are cut in rapidity instead of acollinearity and there is a cut on the minimum visible energy in the event.

Rapidity vs Acollinearity

The t-channel photon exchange produces a long tail in the distribution of the initial state energy loss, since the cross section diverges as the momentum transfer, $-t$, goes to zero. In the extreme case, these events do not appear in the detector, the electron and positron going down the beam pipe opposite a hard photon. A cut on the data, whether in rapidity or acollinearity, to limit the initial state radiation loss needs careful consideration.

The acollinearity cut of the official lepton analysis is replaced by a longitudinal

rapidity cut here, where rapidity η is defined by

$$\eta \equiv \frac{1}{2} ln\left(\frac{\frac{1}{\sin\theta_1} + \frac{1}{\sin\theta_2} + \cot\theta_1 + \cot\theta_2}{\frac{1}{\sin\theta_1} + \frac{1}{\sin\theta_2} - \cot\theta_1 - \cot\theta_2}\right)$$

for θ_i the lab angle of final state fermion i. This variable is just an angle dependent acollinearity, or if you like, acollinearity is just an angle dependent rapidity (see fig. 1). Most importantly, η is a variable truly related to initial state radiation in a manner independent of $\cos\theta'$, the collision frame scattering angle [8,9,5] which is related to the lab angles by

$$\sin^2\theta' \equiv \frac{2\sin\theta_1 \sin\theta_2}{1 - \cos(\theta_1 - \theta_2)}.$$

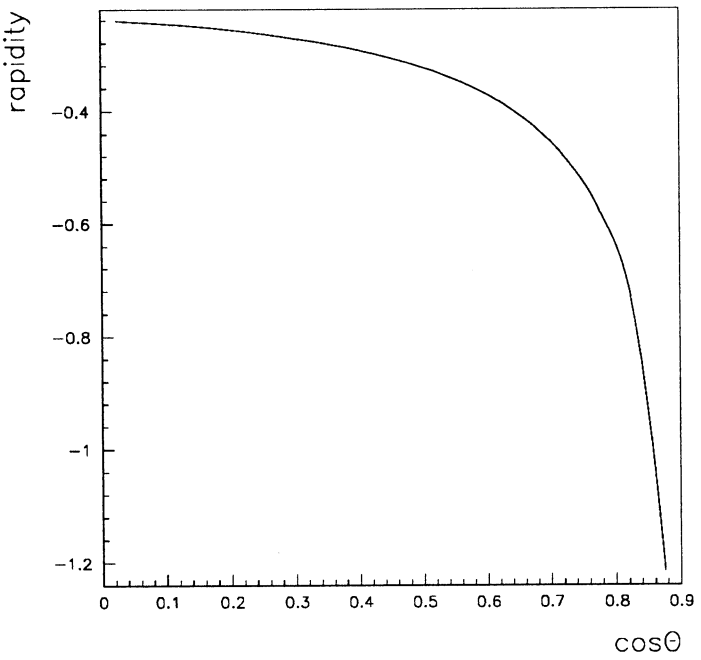

Figure 1: *Rapidity vs* $\cos\theta_{lab}$ *for fixed* 25° *acollinearity*

At $\cos\theta' = 0.9$, a 25° acollinearity cut nearly exceeds the kinematic limit, reaching to within 6.8° of the beam. Clearly, it is the edges of the ALEPH detector in the lab polar angle which limit the phase space of the measurement and not the

cuts themselves, making the definition of the phase space complicated. A rapidity cut of 0.3 does not suffer this problem as can be seen in figure 2, where $|\cos\theta_{lab}|$ is plotted for all tracks in 250000 Bhabha events with $|\cos\theta'| < 0.9$ and $|Y| < 0.3$. No tracks are observed beyond $|\cos\theta_{lab}| = 0.95$, the TPC limit. Thus this combination of cuts produces by themselves a precise phase space definition. Data analysis with such variables minimizes the distortions of the true angular distribution. For this reason, the data here are binned in the collision rest-frame scattering angle with a rapidity cut.

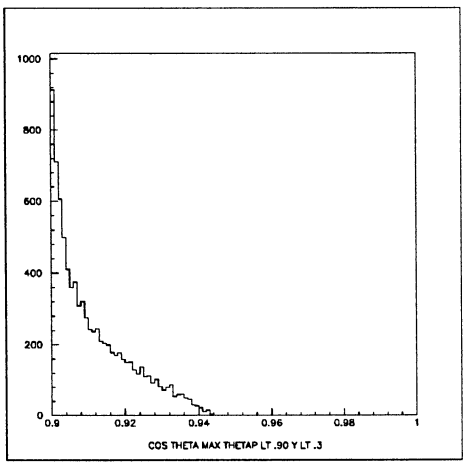

Figure 2: $\cos\theta_{lab}$ *distribution for rapidity cut*

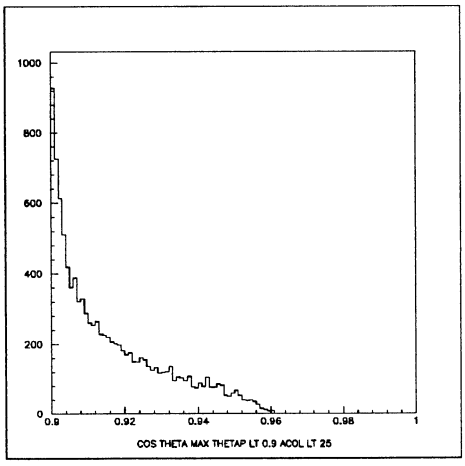

Figure 3: $\cos\theta_{lab}$ *distribution for acollinearity cut*

A second reason to cut on either acollinearity or rapidity is to reduce the $\gamma\gamma$ background. To examine the relative merits of the alternatives, a comparison is made of the efficiency as a function of the background to signal ratio for the two methods using the standard ALEPH $\gamma\gamma$ Monte Carlos and KORALZ muon events. Figure 4 shows the comparison and clearly, for any value of background to signal, the rapidity cut is more efficient (the higher curve).

The third reason for choosing the rapidity cut is that its effect is simply calculated within the fitting program, reducing the reliance on detector simulations. In the collinear radiation approximation, where X_1 and X_2 represent the fractional energies of the beam particles after initial state radiation, the cross section can be calculated from a convolution integral as

$$\left.\frac{d\sigma}{d\cos\theta'}\right|_S \equiv \int dX_1 dX_2 D(X_1,S)D(X_2,S)\frac{d\sigma(SX_1X_2,\cos\theta')}{d\cos\theta'}$$

with

$$\sigma(S) \equiv \int d\cos\theta' \frac{d\sigma}{d\cos\theta'}.$$

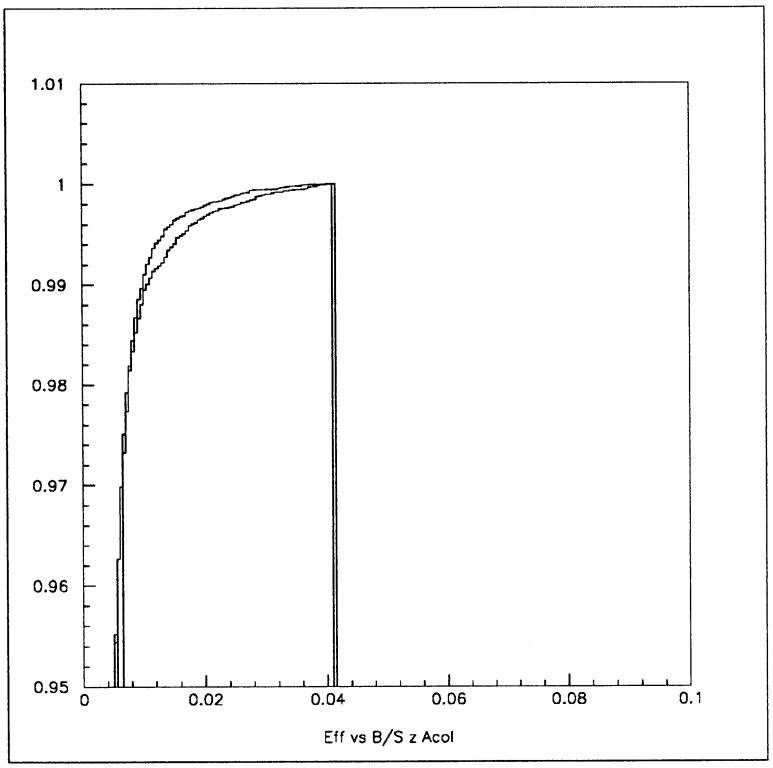

Figure 4: *Efficiency vs Background/Signal*

Introducing the reduced fractional center-of-mass energy squared χ, with

$$\chi \equiv X_1 X_2,$$

and the orthogonal variable, rapidity Y,

$$Y \equiv \frac{1}{2} ln(\frac{X_1}{X_2}),$$

a change of variables (with unit Jacobian) gives

$$\left.\frac{d\sigma}{d\cos\theta'}\right|_S \equiv \int d\chi \frac{d\sigma(S\chi, \cos\theta')}{d\cos\theta'} \int dY D(\sqrt{\chi}e^Y, S) D(\sqrt{\chi}e^{-Y}, S),$$

or

$$\left.\frac{d\sigma}{d\cos\theta'}\right|_S \equiv \int d\chi \frac{d\sigma(S\chi, \cos\theta')}{d\cos\theta'} H(\chi, S),$$

where the flux factor, $H(\chi, S)$, which in the s-channel is independent of θ', is

$$H(\chi, S) \equiv \int dY D(\sqrt{\chi}e^Y, S) D(\sqrt{\chi}e^{-Y}, S).$$

When the integral in $H(\chi, S)$ is extended to the kinematic limits ($Y = \mp ln(\chi)$), the flux factors are equivalent to the published values[2] for the s-channel processes. Note that rapidity is also given by

$$Y \equiv \frac{1}{2} ln\left(\frac{E_{tot} + P_{z\ tot}}{E_{tot} - P_{z\ tot}}\right),$$

which by energy conservation and application of the collinear radiation approximation to the final state implies

$$Y \equiv \eta.$$

The limits of the rapidity integral are given either by the kinematic limit, $\frac{1}{2} ln(\chi)$, or by the cut value. It is clear from the above expressions that a rapidity cut doesn't affect the angular distribution.

Minimum Energy Cut

The second difference in the cuts concerns the minimum energy required of the events. Here again, the emphasis is on reducing the reliance on simulations. The problem arises because the photon exchange amplitudes diverge as s or $-t$ go to zero. This effect maximizes the impact of the radiator functions, the D's and H's, at the limits of phase space where uncertainties are large and where the largest differences between the radiator in the Monte Carlo and the radiatior function in the fitting program might be expected. The official analysis extrapolates the leptonic s-channel cross sections to the fermion threshold. This adds as much as 1% of unobservable cross section to the total cross section, which must then be subtracted in the fitting procedure. This can be avoided by requiring a minimum value for the visible energy seen by the detector, as is done for the hadronic event selection. In the present selection, the visible energy cut is applied to the data, the Monte Carlo when evaluating efficiencies, and in the fitting program in a consistent manner.

Event Sample

Other differences from the standard event selections beyond the two already described are historical. The Bhabha identification differs slightly from that described in the recent ALEPH note by R. Clifft and E. Locci. The effect of the present selection criteria can be seen to be equivalent to the standard algorithm, as is discussed later. In this analysis the sum of the two most energetic tracks plus their associated ECAL and HCAL clusters (in the vicxinity of ECAL cracks), plus the highest energy neutral cluster opposite the highest momentum track, must be greater than 1.11 times the incident energy. The extra muons which pass this cut are eliminated

by requiring that the higher ratio of E/p for the two tracks exceed 0.5, where E is the sum of the charged calorimeter clusters (including the HCAL if there are cracks in the vicinity) and p is the momentum. Taking the common lepton sample and separating out the Bhabhas, the highest efficiencies are attained for this analysis, as none of the problems with μ/τ separation arise and no individual event appears in more than one sample. Furthermore, misidentification probabilities are properly accounted for in the fits.

The event samples obtained are shown in the table below, uncorrected for backgrounds or efficiencies.

Energy	Lcal	Hadrons	$\mu + \tau$	Bhabhas	Total Common Leptons
88.250	13456	2216	188	418	606
89.250	14204	4329	406	569	975
90.250	11962	8102	678	727	1405
91.250	94713	108506	9106	6683	15789
92.250	13667	11535	953	645	1598
93.250	14767	7298	636	481	1117
94.250	15544	5068	473	382	855

Efficiency and Smearing Corrections

The calculation of the efficiencies for the present analysis has been evolving with time. Previously, the effects of missing neutral energy (γ, ν, π^0) were completely absorbed in the efficiency along with the detector and algorithm effects by analyzing the Kingal-Galeph-Julia MC output files on ALWS. It was subsequently realized that the resolutions in both $\cos\theta'$ and Y are in fact energy dependent and hence the corrections must be calculated at each energy. The new efficiency for a given channel (e,μ, τ) contributing to a given sample (e, $\mu+\tau$) is computed as the product of two numbers.

The first efficiency, $A(\cos\theta')$, is the ratio of the number of MC events which pass the $(e, \mu+\tau)$ selection in a given bin of $(|Y| < Y_{cut}, \cos\theta')$, where $\cos\theta'$ and Y are evaluated with the reconstructed tracks, divided by the number of events in the corresponding $(|Y| < Y_{cut}, \cos\theta')$, bin where the variables have been evaluated with the generated momenta of the stable charged particles (thus only using the 'seen' daughters of τ decays). There is also a cut on the scaled invariant mass of the stable charged particles in the generator sample. $A(\cos\theta')$ then, is just the geometrical acceptance, i.e., the corrections due to losses from detector cracks and edges and the effects of detector material.

The second factor, $B(E, \cos\theta')$, is determined at the generator level and so can

be calculated with high statistics. It is the ratio of the number of events in a bin of $(|Y| < Y, \cos\theta')$ just as calculated in the denominator of $A(\cos\theta')$, divided by the number of events in the corresponding bin of $(|Y| < Y, \cos\theta')$ where the true values of the parameters are used, with cuts on the collision rest-frame Y and S'/S_{beam}, i.e., just the phase space of EXPOSTAR. These 'true' values are evaluated with the generated leptons (e,μ,τ) but with the 4-momenta of the final state photons added in. The photons are associated with the fermion legs by the same algorithm used in KORALZ in its rejection calculation (subroutine SKONTY), where the photons are assigned to the fermion legs with which they make the minimum invariant mass.

In the product of these two efficiencies, the intermediate phase space divides out, leaving just the pieces which extrapolate the phase space of the cuts into the phase space of the fitting program. An additional inefficiency of 0.002 is applied to correct for the TPC readout errors as deduced from event scanning [10]. The table below shows typical values for A and B. The sum of the efficiency for a lepton to be correctly identified and the efficiency for the same lepton to be incorrectly classified was always very close to 1.0, for all angles and leptonic channels.

lepton type	A_e	$A_{\mu,\tau}$	B(-0.85)	B(0)	B(.85)
μ	0.0010	0.9990	0.995	1.00	0.995
τ	0.0250	0.9750	0.955	0.96	0.955
e	0.9975	0.0025	0.995	1.00	0.998

For the e sample, the forward smearing efficiencies ($B(\cos\theta' > 0.5)$) were calculated with BHABMC, while the backward efficiencies used the KORALZ μ values. Using the KORALZ μ values for the forward region changed the top quark mass determination by $\leq 1\%$, a negligible fraction of the fit error.

Statistical Treatment in the Fits

The fitting is based on the MINUIT program. The function which is minimized is -2 times the log likelihood, based on normalized Poisson statistics, for the data samples, with χ^2 terms added to allow for the systematic errors. By using log likelihood, and hence passing the correlations through fit parameters, there is no need for a covariance matrix and the resulting confusion which often accompanies its formulation. For each of the event samples, (luminosity Bhabhas, hadrons, $\mu + \tau$, and wide-angle Bhabhas) the expected number of events is computed as

$$N_i^{expect} \equiv L(E) * \left[\sum \sigma_j(E, \cos\theta') * \varepsilon_{ij}(E, \cos\theta')\right] * \kappa_i + BG_i,$$

where L is the luminosity, ε is the efficiency, κ is the systematic multiplier and BG the background to sample i. The correlation due to the finite number of luminosity

Bhabha events are included since the luminosities are also fit parameters. There are systematic multipliers for each data sample, which are also fit parameters.

The sum over cross sections mainly applies to the divided common lepton sample where the misidentification probabilities are the 'efficiencies' for leptons to end up in the wrong category. The τ background to the hadron data sample is also treated this way but without the systematic multiplier applied. The calculation of the expected number of leptons is also properly binned in $\cos\theta'$. The LCAL cross section has the standard Electroweak corrections applied according to ALEPH note 89-124.

The systematic multipliers require that additional terms be added to the χ^2. These take the form

$$\Delta\,\chi^2 \equiv \left(\frac{1\ -\kappa_i}{\delta\kappa_i}\right)^2 .$$

The values of the systematic uncertainties $\delta\kappa$ used for the LCAL cross section, the hadron event selection and backgrounds, and the leptonic selection and backgrounds were 1.34%, 0.6% and 0.5% respectively. An additional systematic error was applied to the Bhabha cross section amounting to 0.7% of the t-channel, varying as $(1 - \cos\theta')^{-2}$. It was inconsequential.

Up to three external measurements may be included in the fits. These are the ALEPH determination of $\alpha_s(M_z^2)$, the CDF determination of M_w, and the ratio of M_w/M_z determined by UA2. The internal QCD fit parameter in the fitting program is the number of colors N_c (for convenience), so including the $\alpha_s(M_z^2)$ measurement requires some care. A term was added to the total χ^2 given by

$$\Delta\,\chi^2 \equiv \left(\frac{QCD_{expostar}\ -\ QCD_{ALEPH}}{\delta\ QCD_{ALEPH}}\right)^2$$

where

$$QCD_{expostar} \equiv N_c\Big(1\ +\ \alpha_{s\ expostar}(M_z^2)/\pi\Big)$$

$$QCD_{ALEPH} \equiv 3\Big(1\ +\ \alpha_s^{ALEPH}/\pi\ +\sqrt{2}(\alpha_s^{ALEPH}/\pi)^2\Big)$$

and

$$\delta\ QCD_{ALEPH} \equiv 3\left(\frac{\delta\alpha_s^{ALEPH}}{\alpha_s^{ALEPH}}\right)(\alpha_s^{ALEPH}/\pi)\Big(1\ +2\sqrt{2}(\alpha_s^{ALEPH}/\pi)\Big),$$

with $\alpha_s^{ALEPH} \pm \delta\alpha_s^{ALEPH} = 0.121 \pm 0.008$. This constrains the QCD final state corrections used in the program to be consistent with those from the ALEPH measurements. A typical value of N_c which results from fits which use this QCD constraint is $N_c = 3.004 \pm 0.007$, indicating that the existing EXPOSTAR calculation is already quite consistent with the ALEPH measurement.

Backgrounds

The relevant backgrounds in the data samples are the same for both the present and the official analysis. The cosmic ray background affects the μ,τ sample and was determined by rerunning this event selection with the same data now requiring that the $|z|$ position of the tracks be between 15 and 40 cm. This background was then scaled by luminosity and reduced to account for the different $|z|$ window. None of the events passed the electron identification. The total number of events added at all energies is 6.4. The $\gamma\gamma$ (leptonic and hadronic) and hadronic backgrounds to the leptons were evaluated by running the analysis on the standard Monte Carlo files on ALWS. There were no backgrounds to the Bhabha sample. The calculated backgrounds to the $\mu+\tau$ sample were binned in $\cos\theta'$. This hadronic background was calculated from the generated MC files properly scaled to reflect the observed hadronic cross sections. The $\gamma\gamma$ background was scaled to the luminosity. The $\gamma\gamma$ and τ backgrounds to the hadronic sample are the same as were prepared for Singapore.

Description of Fits and Fit Results

The fit parameters of the EXPOSTAR calculations are the Z mass, the top mass, the Higgs mass, the number of νs, the number of colors, and three scale factors for the vector, axial, and overall leptonic weak couplings. Most of this discussion will concentrate on fits for the Z mass, the top mass and the number of colors. The Higgs mass was fixed at 100 GeV. The data samples that can be fit include any combination of the following: the number of observed LCAL events, the number of TPC selected hadrons, the number of common leptons in the μ,τ sample, in bins of $\cos\theta'$ or integrated over $\cos\theta'$, and the number of common leptons in the Bhabha sample again in bins of $\cos\theta'$ or integrated over $\cos\theta'$. Any of the three external measurements can also be included.

The EXPOSTAR calculation package has been updated to include the $\gamma-\gamma$ boxes and the $Z-\gamma$ boxes in the s and t-channels and s-t cross terms. It is believed that this now includes all large ($> 0.3\%$) contributions to the following processes:

$$\sigma^{had}_{tot}, \left.\frac{d\sigma}{d\cos\theta}\right|_{\mu,\tau}, \left.\frac{d\sigma}{d\cos\theta}\right|_{e^+e^-}, \left.\frac{d\sigma}{d\cos\theta}\right|_{\tau_{l,\tau}}, \sigma^{had}_{tot,left} - \sigma^{had}_{tot,right}.$$

The b and c quark forward backward asymmetries have not had the photonic boxes added at this time. A more complete description of the calculations is found in the appendix.

The fitting program was written so that many different combinations of data samples could be fit. This is accomplished with logical data cards. In addition, the

range of energy points and angular bins (for the μ, τ sample and the Bhabha sample separately) can be selected by data cards. The consistency between the different data samples is indicated by the statistical consistency of the results shown in the following table. Note the wide variety of fits which can be made. One interesting result is that the fit converges to the same minimum whether the forward piece of the Bhabha events is included or not.

N_{had}	$\frac{dN_{\mu,\tau}}{d\cos\theta'}$	$\frac{dN_e}{d\cos\theta'}$	M_w	α_s	M_z	M_{top}	N_{col}	$\chi^2/N.D.F.$
X	$X\|_{-.9}^{.9}$	-	-	-	91.176 ± 0.010	141^{+68}_{-117}	3.020 ± 0.030	131/130
X	-	$X\|_{-.9}^{.9}$	-	-	91.175 ± 0.010	203^{+66}_{-107}	2.970 ± 0.040	109/130
X	-	$X\|_{-.9}^{.5}$	-	-	91.175 ± 0.010	194^{+74}_{-135}	2.980 ± 0.040	78/105
X	$X\|_{-.9}^{.9}$	$X\|_{-.9}^{.9}$	-	-	91.177 ± 0.010	163^{+58}_{-94}	3.000 ± 0.027	240/256
-	$X\|_{-.9}^{.9}$	$X\|_{-.9}^{.9}$	-	-	91.189 ± 0.024	175^{+72}_{-175}	2.990 ± 0.036	237/249
X	$X\|_{-.9}^{.9}$	$X\|_{-.9}^{.9}$	-	X	91.177 ± 0.010	163^{+50}_{-73}	3.004 ± 0.008	240/257
X	$X\|_{-.9}^{.9}$	$X\|_{-.9}^{.9}$	X	X	91.176 ± 0.010	141^{+38}_{-47}	3.005 ± 0.007	240/259

An additional fit was performed to see if the data preferred a form different than that predicted by the Standard Model. The fit variables were M_Z, N_ν, N_c, and the vector and axial lepton coupling multipliers. The results are shown below.

M_Z	N_ν	N_c	k_v	k_a	$\chi^2/N.D.F.$
91.177 ± 0.010	2.95 ± 0.11	3.03 ± 0.035	1.09 ± 0.27	1.002 ± 0.005	239/254

These results show that the Standard Model with 3 light neutrinos describe the data well.

A fit to the hadronic cross sections determined in the energy scan, relative to the hadronic cross section at the peak, can be made with EXPOSTAR. Many systematic errors cancel in these ratios, an advantage when results from different experiments are combined. The nature of this fit is such that a χ^2 evaluation is required, with the appropriate covariance matrix. The correlations are simple functions of the numbers of events so that the covariance matrix is simple to calculate. Using just the numbers of hadrons and luminosity Bhabhas, and assuming $N_\nu = N_c = 3$, the results from such a relative fit to the ALEPH data are shown in the table below. The results are in agreement with the previous fits. For example, such a fit would have produced results inconsistent with the other fits had the incorrect vacuum polarization been used in the luminosity Monte Carlo.

M_Z	M_{top}	$\chi^2/N.D.F.$
91.175 ± 0.011	163^{+53}_{-90}	1/4

A similar fit but using also information in the ratio $R = \sigma_h/\sigma_l$ across the scan and the published ALEPH value of α_s, gives the following results, assuming $N_\nu = 3$.

M_Z	N_c	M_{top}	$\chi^2/N.D.F.$
91.177 ± 0.011	3.006 ± 0.008	166 ± 61	7/10

Conclusions

We have fit the 1990 ALEPH data directly with a Standard Model calculation[1]. All of the fits to any of the data samples produce acceptable results which are consistent within all sets of fits. The best value of the top quark mass using ALEPH data alone is $m_t = 163^{+50}_{-73}\ GeV/c^2$. If we extend the fit beyond the minimal Standard Model, we find the number of neutrinos to be 2.95 ± 0.11 and the vector and axial leptonic couplings to be consistent with the Standard Model predictions.

Appendix A: Comparison of ALIBABA and EXPOSTAR

The t-channel calculation of the EXPOSTAR and ALIBABA programs have been compared and found to be in agreement to within 0.5% (at worst). The comparison is non-trivial due to the different cuts used by the two programs. ALIBABA cuts in the observed variables of the final state leptons: momentum, lab angle and polar acollinearity. EXPOSTAR cuts in the collision rest-frame variables: rapidity, invariant energy, and scattering angle. A comparison between the two requires the use of a Monte Carlo event generator where both sets of cuts can be applied to a common event sample. The best wide angle event generator available is BHABMC (Kleiss and Hollik), but it only calculates at order α. The two semi-analytic Bhabha calculations calculate to order α^2 with exponentiation. Hence, a rigorous comparison is not possible, but limits can be determined.

If the BHABMC is run in the t channel only, the ratio R of the number of events passing the ALIBABA cuts ($P_{min} > 1\ GeV, |\cos\theta_{lab}| < 0.9, acol < 25°$) to the number of events passing the EXPOSTAR cuts ($|Y| < 0.3, \chi > 0.005, |\cos\theta'| < 0.9$) is found to be 0.945. The deviation of this ratio from 1 is due just to radiative corrections. If this deviation is assumed to be fully correlated to the cross section, then an upper limit of the value of R that would be found for an order α^2, exponentiated calculation can be approximated from the relation

$$\frac{1 - R_{\alpha^2,\ exponentiated}}{1 - R_{\alpha,\ unexponentiated}} \approx \frac{\sigma_{born} - \sigma_{\alpha^2,\ exponentiated}}{\sigma_{born} - \sigma_{\alpha,\ unexponentiated}}.$$

The right-hand side can be computed using the ALIBABA program, as it has as an option the capability to compute to order α, unexponentiated. Since both ALIBABA and EXPOSTAR find $\sigma_{born} = 556.6$ pb, the relation implies $R_{\alpha^2,\ exponentiated} < 0.956$. With the order α ratio from the BHABMC results, the range of $R_{\alpha^2,\ exponentiated}$ is given by

$$0.945 < R_{\alpha^2,\ exponentiated} < 0.956.$$

The observed ratio of the two calculations for the two sets of cuts is 0.949.

Appendix B: Technical description of the EXPOSTAR calculations

The statistical precision of data coming from e^+e^- colliders will soon reach the point where the extraction of the fundamental electroweak parameters could be limited by the accuracy of the functional description of the Standard Model used in fitting the data. While accurate numerical calculators exist [1], all depend on time-consuming Monte Carlo numerical integrations, a form entirely too cumbersome to be used with numerical fitting programs such as MINUIT [3]. In order to overcome this difficulty, we have adapted the EXPOSTAR Monte Carlo [1] so that it can be used with MINUIT to fit data with the Standard Model.

Important correlations existing in both the data and the theoretical expressions imply that a global fit to many simultaneous Standard Model processes is needed. Such a fit more correctly tests the validity of the Standard Model. The internal consistency of the theoretical calculations must be strictly maintained to insure that the consequences of parameter variations are correctly manifested in the comparison of the computed observables with data. While the rigor of the numerical evaluations of the minimal Standard Model is essential, accurate convergence to solutions outside the Standard Model must be allowed.

Data analysis requires that cuts be applied to data to eliminate backgrounds and to avoid regions of low detection efficiency. If the computed cross sections include the phase space reductions due to these cuts, they depend less on Monte Carlo estimated corrections. Due to the large number of cross sections that need to be evaluated in the course of a fit, the speed of calculation is of utmost importance. Also, a simple, straightforward interface is required, since many different fits must usually be performed to arrive at a proper systematic understanding of the results.

Within the computational scheme of the program, three cuts define the phase space of the differential cross sections. The choice of variables is predicated on the computational scheme. As in the EXPOSTAR Monte Carlo, the collinear radiation

approximation is used. This assumption allows the computation of a cross section as a convolution integral of the electron structure functions, i.e., the probability densities of the beam lepton energies after initial state radiation, with invariant cross sections evaluated at a reduced energy. As these bare cross sections are invariant they can be evaluated in the rest-frame of the collision where the kinematics are simple. This technique has long been used in the analysis of hadronic experiments [8,9], but has only recently has been applied to e^+e^- interactions [5]. With S the center-of-mass energy squared and X the beam leptons fractional energy after initial state radiation, the differential cross section is written as

$$\left.\frac{d\sigma}{d\cos\theta'}\right|_S \equiv \int dX_1 dX_2 D(X_1,S)D(X_2,S)\frac{d\sigma(SX_1X_2,\cos\theta')}{d\cos\theta'} + BOX_{Z\gamma,\gamma\gamma}$$

and the total cross section as

$$\sigma(S) \equiv \int d\cos\theta' \frac{d\sigma}{d\cos\theta'} + BOX_{Z\gamma,\gamma\gamma} ,$$

where $BOX_{Z\gamma,\gamma\gamma}$ is the order α sum of photonic box and bremsstrahlung diagrams not absorbed in the structure functions.

Introducing the fractional reduced C.M. energy χ where

$$\chi \equiv X_1X_2$$

and the rapidity Y,

$$Y \equiv \frac{1}{2}ln(\frac{X_1}{X_2}),$$

gives

$$\left.\frac{d\sigma}{d\cos\theta'}\right|_S \equiv \int d\chi \frac{d\sigma(S\chi,\cos\theta')}{d\cos\theta'} \int dY D(\sqrt{\chi}e^Y,S)D(\sqrt{\chi}e^{-Y},S)$$

or

$$\left.\frac{d\sigma}{d\cos\theta'}\right|_S \equiv \int d\chi \frac{d\sigma(S\chi,\cos\theta')}{d\cos\theta'} H(\chi,S),$$

where, when the integral extends to the kinematic limits ($Y = \mp ln(1-\chi)$) the flux factor $H(\chi,S)$ is just that in the literature [2],

$$H(\chi,S) \equiv \int dY D(\sqrt{\chi}e^Y,S)D(\sqrt{\chi}e^{-Y},S).$$

Extending the collinear radiation assumption to the final state implies that final state radiation leaves the directions of the final state fermions unchanged. When the 4-momenta of the final state radiation is added to the 4-momenta of the appropriate final state fermion, their transverse momenta will exactly balance. Then, with $\sin\theta$ positive, in the lab-frame find

$$S\chi \equiv M^2 \equiv 2P_1P_2(1-\cos(\theta_1-\theta_2)) \equiv 2P_T^2\frac{(1-\cos(\theta_1-\theta_2))}{\sin\theta_1\sin\theta_2}$$

and in the collision rest-frame

$$S\chi \equiv \frac{4P_T'^2}{\sin\theta'^2}.$$

Hence

$$\sin^2\theta' \equiv \frac{2\sin\theta_1\sin\theta_2}{1-\cos(\theta_1-\theta_2)}.$$

This is just the ratio of the invariants, with respect to longitudinal boosts, Sχ and P_T^2. Also, since Y, the longitudinal rapidity is defined as

$$Y \equiv \frac{1}{2}ln(\frac{X_1}{X_2}) \equiv \frac{1}{2}ln(\frac{E+P_z}{E-P_z}),$$

which can then be written as

$$Y \equiv \frac{1}{2}ln[\frac{P_T((\frac{1}{\sin\theta_1}+\frac{1}{\sin\theta_2})+(\cot\theta_1+\cot\theta_2))}{P_T((\frac{1}{\sin\theta_1}+\frac{1}{\sin\theta_2})-(\cot\theta_1+\cot\theta_2))}].$$

So rapidity is just a function of the two observed polar lab angles of the final state leptons.

A cut in rapidity constitutes an angle-dependent acollinearity cut (useful for eliminating $\gamma\gamma$ backgrounds from lepton final states) which, in the collinear radiation approximation, leaves the $\cos\theta'$ distribution unaffected. A rapidity cut is in fact more effective at eliminating $\gamma\gamma$ background than is an acollinearity cut since it is effective at all angles, while acollinearity cuts only remove backgrounds near 90°. Further, the effect on the phase space of such a cut can be calculated explicitly without recourse to a Monte Carlo (although this correction can be calculated with an event simulator). By making simultaneous cuts in $\cos\theta'$ and rapidity, the phase space corresponding to regions of low efficiency, e.g., the beam pipe region, can be excluded from the region of phase space used to calculate cross sections. For instance, the ALEPH detector has tracking coverage up to $\cos\theta_{lab} = 0.95$ and if $|\cos\theta'| < 0.90$, and $|Y| < 0.3$, then the fraction of Z° decays to muons for which either lepton has $|\cos\theta_{lab}| > 0.95$ is less than 10^{-6}.

A third cut is made which requires a minimum value for the square of the visible mass, including final state radiation. This constitutes the lower limit of integration of the χ integral. As long as this cut is at a small value (< 0.1) the calculation is insensitive to it to the level of typical experimental accuracies (0.2%), provided it is high enough to exclude the region where the divergent photon exchange piece dominates, ($\chi > 0.005$), corresponding to visible mass cuts between 6 and 29 GeV at the Z°, as $\chi \approx (E_{seen}/2E_{beam})^2$.

Construction of Bare Cross Sections

The bare cross sections are constructed using the * scheme [1] of absorbing the electroweak radiative corrections. As the experimental cross sections can be easily evaluated in the collision rest frame by simply binning the data in $\cos\theta'$, many computational simplifications are achieved, the most powerful being for the Bhabha cross section. The bare (ignoring initial state radiation) unpolarized μ and τ cross sections are defined as follows:

$$\mu\ ,\ \tau\ :\ \left.\frac{d\sigma}{d\cos\theta'}\right|_{S'} \equiv \frac{\alpha^2(S')}{4S'}\frac{1}{2}\sum_{i=1}^{i=2}\sum_{j=1}^{j=2}|A_{ij}(S',\cos\theta')|^2(1+\frac{4}{3}Q^2\frac{\alpha_o^2}{\pi})$$

where the $A_{ij}(S',\cos\theta')$ are the polarized amplitudes. For example the left-left (meaning left-handed electrons on unpolarized positrons producing polarized left-handed μs) is:

$$A_{ll}(S',\cos\theta') \equiv (\frac{U'}{S'})(\frac{Q_{el}(S')Q_{\mu l}(S')}{1-\Pi_{\gamma\gamma}(S')} + R(S')C_{el}(S')C_{\mu l}(S') + BOX_{wll}(S'))$$

where

$$\begin{aligned} R(S') &\equiv \frac{1}{4\sin^2\theta^*\cos^2\theta^*}\frac{S'}{S'-M_z^2\ +\ \Pi_z(S')} \\ &\equiv \frac{1}{4\sin^2\theta^*\cos^2\theta^*}\frac{S'}{S'-M_z^{2*}+iIm(\Pi_z(S))} \end{aligned}$$

and

$$Im(\Pi_z(S')) \equiv S'\sum_i\frac{\Gamma_i(S')}{\sqrt{S'}} \equiv S'\frac{\Gamma(S')}{\sqrt{S'}},$$

the real part of Π_z being absorbed into M_z^2, making it a q^2 dependent function. Here,

$$\frac{\Gamma(S)}{\sqrt{S}} \equiv \sum_i\frac{\alpha(S)}{24\sin^2\theta^*\cos^2\theta^*}(C_{li}^2(S)+C_{ri}^2(S))(1+\frac{4}{3}Q^2\frac{\alpha_o^2}{\pi})F_i$$

where

$$F_i \equiv (1+\frac{\alpha_s(S)}{\pi})$$

when i corresponds to (u,d,s,c,b) and is 1 otherwise. BOX_w is the contribution of the non-universal [1] parts of the W^+W^- and $Z^\circ Z^\circ$ box diagrams and the angular dependence of the universal [1] parts of the W^+W^- diagrams. The S' dependence of electric and weak couplings (Q and C) is due to the vertex corrections (including relevant top quark mass effects) and the running of $\sin^2\theta^*$. For b quarks, the effect of the phase space reduction due to the large mass of the b quark is included, after rewriting the left-handed and right-handed couplings in terms of the axial and vector couplings

$$2(C_{lb}^2(S)+C_{rb}^2(S)) \equiv (C_{ab}^2(S)\frac{(3-\beta^2)}{2}+C_{vb}^2(S)\beta^2)\beta.$$

The number of colors is introduced as an overall multiplicative factor, N_c, and is a parameter of the EXPOSTAR fits.

The total hadronic cross sections is constructed by replacing the muon polarized charges and couplings by like expressions with appropriate quantum numbers, multiplied by the additional $(1 + \frac{\alpha_s(S)}{\pi})$ QCD factor. The total cross section can then be calculated by replacing

$$(\frac{U'}{S'})^2 \ , (\frac{T'}{S'})^2 \ \equiv \frac{1}{4}(1 \pm \cos\theta')^2$$

by $\frac{8}{3}$ in each of the polarized cross sections for the u,d,s, and c quarks, and a more complicated expression to include the mass effects of the b quark, as was done for the width. The total cross section is then the sum over the 5 quark contributions. The number of colors is treated just as it was in the case of the widths, and is used as a fit variable to change the hadronic width.

The complicated angular behavior of BOX_w and $BOX_{Z\gamma,\gamma\gamma}$ needs comment. The $BOX_{Z\gamma,\gamma\gamma}$ has been numerically integrated over $\cos\theta'$ and an angular coefficient determined by dividing the integral by the value at $t = -s/4$. This energy dependent factor is used to evaluate the contribution to the total hadronic cross section of these box diagrams during initialization, to allow for different starting values of the input electroweak parameters. The weak box amplitudes are integrated in a similar manner over $\cos\theta'$ with a additional weight of $\frac{3}{8}(1 \pm \cos\theta')^2$, normalized by the value at $t = -s/2$. This angular integration factor multiplied by the initial weak box amplitude produces the correct cross terms in the integrated matrix element.

It is in the discussion of the Bhabha cross section that the importance of defining cross sections in the collision rest-frame becomes most important. Momentum conservation at the vertex in the t-channel graphs mixes the initial and final states and usually destroys the factorization shown in the ansatz (where the cross sections only depend on χ) if the final observed momentum is held fixed. However, here the differential cross sections are being evaluated at fixed rest-frame angle, where the t exchange amplitude is simply

$$T' \ \equiv (P_1' + P_3')^2 \ \equiv \frac{-S'}{2}(1 - \cos\theta') \ \equiv \chi\frac{S(1 - \cos\theta')}{2}.$$

This restores the factorized form of the simple calculation because

$$P_3' \ \equiv (\sqrt{\chi}P_{beam}, \sqrt{\chi}P_{beam}\sin\theta', 0, \sqrt{\chi}P_{beam}\cos\theta')$$

due to momentum conservation in the collision rest-frame. While this is commonly done in calculations of high P_t hadron production [9] to avoid the pole at $T' = 0$, this is the first instance of this technique being applied to Bhabha scattering. The

bare Bhabha cross sections can be obtained from the s-channel calculation through a Fiertz transformation [4] yielding:

$$\left.\frac{d\sigma}{d\cos\theta'}\right|_{S'} \equiv \frac{S'}{8}\sum_{i=1}^{i=2} A_i^2(S',T')(1+\frac{4}{3}Q^2\frac{\alpha_o^2}{\pi}) \; + \; BOX_{Z\gamma,\gamma\gamma}$$

where the sum is over the electron polarizations. $BOX_{Z\gamma,\gamma\gamma}$ is the contribution of the photonic boxes and bremsstrahlung diagrams not included in the structure functions at order α, but now the s, t and s-t cross terms are computed. For example, the left-handed cross section is:

$$\begin{aligned} A_l^2 \equiv \Big|&\frac{\alpha(S')U'}{S'^2}[\frac{Q_{el}^2(S')}{1+iIm(\Pi_\gamma(S'))} + R(S')C_{el}^2 + BOX_{wll}(S')] \\ &-\frac{\alpha(T')}{T'}[Q_{el}^2(T') + R(T')C_{el}^2(T') + BOX_{wll}(T')]\Big|^2 \\ +\Big|&\frac{\alpha(S')U'}{S'^2}[\frac{Q_{el}(S')Q_{er}(S')}{1+iIm(\Pi_\gamma(S'))} + R(S')C_{el}(S')C_{er}(S') + BOX_{wlr}(S')]\Big|^2 \\ +\Big|&\frac{\alpha(T')}{T'}[Q_{el}(T')Q_{er}(T') + R(T')C_{el}(T')C_{er}(T') + BOX_{wlr}(T')]\Big|^2 \end{aligned}$$

where all of the functions of q^2 are as defined for the μ,τ cross sections but evaluated at the appropriate value of q^2 (S' or T'). The BOX_w function in the amplitudes again represents the non-universal residual heavy weak boxes and the angular dependence of the universal part. R(T) differs from R(S) in that

$$R(T) \equiv \frac{1}{4\sin^2\theta^*(T)\cos^2\theta^*(T)}\frac{T}{|T|+M_z^{2*}(T)}$$

because

$$Im(\Pi_z(T)) \equiv 0$$

for the same reason that the $\Pi_\gamma(T')$ is also zero.

The vertex,running coupling, and Z mass functions were written as functions of q^2, and so continue to the spacelike region. In this manner the bare Bhabha cross section can be constructed to the same accuracy (1 loop) as the s-channel processes.

b and c quark Forward Backward Asymmetries

The quark forward-backward asymmetries can be easily constructed from ratios of sums and differences of polarized cross sections. Due to the linearity of these constructs and their definitions, the effects of initial state radiation are included

by calculating the convolutions and forming ratios. Define the helicity sums for opposite and like helicities as

$$\frac{d\sigma_{opp\ b,c}}{d\cos\theta'} \equiv \int d\chi(\frac{d\sigma_{lr\ b,c}}{d\cos\theta'} + \frac{d\sigma_{rl\ b,c}}{d\cos\theta'})H(\chi,S)|_{t=-s/2}$$

$$\frac{d\sigma_{sam\ b,c}}{d\cos\theta'} \equiv \int d\chi(\frac{d\sigma_{ll\ b,c}}{d\cos\theta'} + \frac{d\sigma_{rr\ b,c}}{d\cos\theta'})H(\chi,S)|_{t=-s/2},$$

and form the ratio

$$A(b,c\ quark) \equiv \left(\frac{d\sigma_{sam\ b,c}}{d\cos\theta'} - \frac{d\sigma_{opp\ b,c}}{d\cos\theta'}\right) \Big/ \left(\frac{d\sigma_{sam\ b,c}}{d\cos\theta'} + \frac{d\sigma_{opp\ b,c}}{d\cos\theta'}\right).$$

The angular integration shows $A_{fb}(b,c\ observ)$ to be

$$A_{fb}(c\ observ) \equiv \frac{(1+X)^3+(1-X)^3-2}{(1+X)^3-(1-X)^3}A(c\ quark)$$

and

$$A_{fb}(b\ observ) \equiv \frac{(1+\beta X)^3+(1-\beta X)^3-2}{\beta(6\beta X\ +\ 2(\beta X)^3)}A(b\ quark)$$

where $X = \cos\theta^{max}$. The more complicated expression for b quarks is due to their non-negligible mass.

Polarizations

Similarly the τ polarization asymmetry can be formed by

$$\left.\frac{d\sigma_{\tau\ r}}{d\cos\theta'}\right|_{S,\cos\theta'} \equiv \int d\chi(\frac{d\sigma_{rr\tau}}{d\cos\theta'} + \frac{d\sigma_{lr\tau}}{d\cos\theta'})H(\chi,S)$$

$$\left.\frac{d\sigma_{\tau\ l}}{d\cos\theta'}\right|_{S,\cos\theta'} \equiv \int d\chi(\frac{d\sigma_{ll\tau}}{d\cos\theta'} + \frac{d\sigma_{rl\tau}}{d\cos\theta'})H(\chi,S)$$

using the differential cross sections described in the first process (μ , τ). The polarization asymmetry as a function of S and $\cos\theta'$ is then

$$P_\tau \equiv \left(\frac{d\sigma_{\tau\ l}}{d\cos\theta'} - \frac{d\sigma_{\tau\ r}}{d\cos\theta'}\right) \Big/ \left(\frac{d\sigma_{\tau\ l}}{d\cos\theta'} + \frac{d\sigma_{\tau\ r}}{d\cos\theta'}\right).$$

The beam polarization asymmetries can be formed from the ratio of the difference over the sum of

$$\sigma_r \equiv \int d\chi(\sigma_{rl} + \sigma_{rr})H(\chi,S)$$

$$\sigma_l \equiv \int d\chi(\sigma_{ll} + \sigma_{lr})H(\chi,S)$$

where the cross sections refer to whichever process is being considered.

Initial State Radiation and Flux Factors

The essential ansatz of these EXPOSTAR fits treats the effects of initial state radiation through the convolution of the bare cross sections evaluated at reduced energies with the probability that the initial state electron and positron has radiated away the remaining energy. As the leptonic cross sections are evaluated at fixed $\cos\theta'$, this collinear radiation does not affect the angular distributions.

In the event that a rapidity cut is applied to the data, then the flux factor cannot be taken from the literature directly [2], but the integral over rapidity must be evaluated. The integral has the interesting property that for

$$\chi \leq e^{2Y_{max}}$$

the range of integration is all of phase space and the result must equal the flux factors in the literature, and hence in this case the flux factors are used to improve numerical accuracy.

The structure functions used for the s-channel are taken from reference [2]. For the region where the rapidity cut does not restrict the region of integration, the full flux factor (first form of eq. 8 of reference [2]) is used, also absorbing the non-collinear terms. The rapidity integral is evaluated numerically using the individual electron structure functions from the same source. The numerical integral of the structure functions over the kinematically allowed phase space agrees with the flux factors to better than 1% in the hard radiation region where it must be used.

The efficiency of the rapidity cut can be compared with event-generating Monte Carlos. This was checked for muon pair production with KORALZ [5]. It is observed that the closed form calculation reproduces the Monte Carlo result if the final state radiation is turned off, but a small error is made due to the non-collinearity of the final state radiation. As this error can be calculated, by taking the ratio of efficiencies with and without final state radiation in the Monte Carlo, it can be applied as a correction to the data.

For the wide angle Bhabha cross section the initial state photonic corrections are also absorbed by the use of two structure functions. The scheme adopted multiplies the s-channel amplitude by the square root of the flux factor used for the s-channel calculations and multiplies the t-channel amplitude by a corresponding factor corrected for the different non collinear terms[6], retaining only the leading log for the α^2 correction [7]. The resulting cross term is also consistent with reference [6]. By this mechanism there is no compromise made on the s-channel part of the calculation as it can be treated identically to what has already been described.

The t-channel flux factor and structure functions are written in the second form of eq. 8 of reference [2]. Redefining χ as used there,

$$\chi \equiv 1 \; - \; X_1 X_2,$$

gives

$$H_t(\chi, S) \; \equiv \Delta_t \beta \chi^{\beta-1} \; - \frac{\beta_t}{2}(2-\chi)$$

$$+\frac{\beta_t^2}{8}[(2-\chi)(3ln(1-\chi) - 4ln(\chi)) - \frac{4ln(1-\chi)}{\chi} - (6-\chi)];$$

$$\beta \; \equiv \frac{2\alpha}{\pi} ln(\frac{S}{m^2} - 1);$$

$$\beta_t \; \equiv \frac{2\alpha}{\pi}(ln(\frac{S}{m^2}) + ln(\frac{1-\cos\theta}{2}) - 1) \equiv \frac{2\alpha}{\pi} ln(\frac{|T|}{m^2} - 1);$$

$$\Delta_t \; \equiv 1 + \frac{\alpha}{\pi}(\frac{3}{2}(ln(\frac{|T|}{m^2} - 1) - \frac{\pi^2}{6} - \frac{1}{2} - ln^2(\frac{1-\cos\theta}{2})) + (\frac{\alpha}{\pi})^2(\frac{9}{8} - \frac{\pi^2}{3}) ln(\frac{|T|}{m^2} - 1)^2.$$

The electron structure functions needed to correct for the rapidity cut can be constructed from the above terms in the form of reference [2]. The terms proportional to β_t and β_t^2 cancel the leading logs in the integral

$$\int H_t(\chi, S) d\chi \; \equiv K,$$

where K is the finite remainder due to the non-collinear terms.

References

[1] D.C. Kennedy and B.W. Lynn, Nucl. Phys. **322B** 1 (1989). D.C. Kennedy, B.W. Lynn, C.J.-C. Im, and B. Stuart, Nucl. Phys. **321B** 83 (1989). B. W. Lynn, S. Sylepsky, B. Stuart, D. Levinthal, in preparation.

[2] O. Nicrosini and L. Trentadue, Phys. Lett. **196B** 551 (1987).

[3] F. James and M. Roos, C.E.R.N. Report D506 (1989).

[4] B.W. Lynn, M.E. Peskin and R.G. Stuart C.E.R.N. Report 86-02 Vol 1 90 (1986).

[5] S. Jadach, Z. Was, Phys. Rev. **D41** 1425 (1990)

[6] M. Grecco Riv. d. Nuovo Cim. Vol 11 N5 (1988)

[7] W. Beenakker, F. A. Berends, S.C. Van der Marck Nucl. Phys. B (in Print)

[8] S. Drell, C.N. Yan Phys Rev Let. **25** 316 (1970)

[9] A.L.S Angelis *et al* Nucl. Phys **209B** 284 (1982) D. Levinthal Ph.D. thesis Nevis Report 234 Columbia Univ. (1980)

[10] H. Meinhard, ALEPH Note 90-170, 28 Nov 1990